Science AAAS

Spin Rate of Asteroid (54509) 2000 PH5 Increasing Due to the YORP Effect

Patrick A. Taylor, *et al.*

Science **316**, 274 (2007);
DOI: 10.1126/science.1139038

was extracted from each individual imaging data set (*13*), and the resulting light curves were grouped according to date; all the 2001 and 2002 light curves were taken together, then all the 2002–2003, 2003–2004, and 2004–2005 data, so that each data set had a 1-year time base. To find changes in the sidereal period, we shifted the observation times of the data points within each combined set by the established phase angle bisector (PAB) approximation (*13*, *14*), which requires knowledge of the spin-axis orientation. Using a combination of radar data and our optical light curves, Taylor *et al*. (*12*) report that the pole position resides within 10° of (180°, –85°) in ecliptic coordinates (J2000).

Fourier analysis of the light curve modulation was then performed separately for each time-corrected data group (*13*) to determine the yearly averaged sidereal rotation periods (Table 1). The light curve amplitude changed little within any data set because of the nearly constant aspect angle of the asteroid throughout the observations. As a result of the asteroid's shape, there was also a pronounced asymmetry in the light curve that ultimately allowed unambiguous phasing of the data (Fig. 1). Sidereal rotation periods P were determined from 2001 to 2005 and were seen to decrease at a linear rate, with a fractional change of -1.7×10^{-6} (±9%) per year; that is, the asteroid has been increasing its rotation rate ω over these 4 years by $d\omega/dt = 2.0\ (\pm 0.2) \times 10^{-4}$ degrees day^{-2} (Fig. 2). This result was confirmed from analysis of the combined light curve and radar data in (*12*). Detailed dynamical simulations that used the shape model in (*12*) were performed that reproduced the close Earth approaches from 2001 to 2005, from which we can rule out Earth-tug effects as a potential mechanism for the observed sidereal-period decrease (Fig. 2) (*13*). Moreover, there is no reason for Earth tugs to be coherent, so uncorrelated positive and negative shifts in spin rate are possible in subsequent years. The reasonable agreement between observations and YORP simulations (*12*) and the fact that planetary tugs cannot account for the observed effect leaves YORP as the only viable cause.

The fast rotation of PH5 could imply that this asteroid underwent significant YORP evolution in the past. Indeed, its obliquity near 180° supports this idea because it is near one of the asymptotic YORP regimes (*11*, *15*). Our result suggests that it would take ~550,000 years for YORP to double the rotation rate of PH5 in the future. From this value we may expect that YORP will cause structural changes, mass shedding, or even fission of this object at some point in the future, depending on its internal strength. To investigate this possibility, we ran a simulation that numerically propagated the orbit of PH5 and 999 close clones (*13*). We found a median dynamical lifetime before particle removal from the simulation, by solar or planetary impacts, of ~15 million years (My), a surprisingly long time scale (Fig. 3). The longest-lived clones of PH5 (about 6%) survived 100 My of orbital evolution. In a second step, we numerically integrated the secular evolution of the spin state for each of these 1000 particles along their precise orbits (*13*), with the YORP strength set to our observed value. At 35 My, when 25% of the original clone population remained, the median rotation period was 19 s with a lowest extreme of 5 s (Fig. 3).

Our observational calibration of the YORP effect, in conjunction with orbital and spin integrations, demonstrates that asteroids like PH5 can attain extremely fast rotation rates. Our work also implies the possible existence of a population of 100-m asteroids with rotation periods of ~20 s, significantly faster than the most rapidly rotating asteroid of this size, 2000 WH10 with $P \sim 80$ s (*16*). Light curve observations to date are biased against the detection of such short periods, and hence the number of such bodies is unconstrained at present. If no such objects are found, then the most likely explanation is eventual significant mass shedding or rotational fission before they reach this value of P.

References and Notes

1. D. P. Rubincam, *Icarus* **148**, 2 (2000).
2. S. M. Slivan, *Nature* **419**, 49 (2002).
3. D. Vokrouhlický, D. Nesvorný, W. F. Bottke, *Nature* **425**, 147 (2003).
4. D. Vokrouhlický, M. Broz, W. F. Bottke, D. Nesvorný, A. Morbidelli, *Icarus* **182**, 118 (2006).
5. S. R. Chesley *et al.*, *Science* **302**, 1739 (2003).
6. A. Morbidelli, D. Vokrouhlický, *Icarus* **163**, 120 (2003).
7. P. Pravec, A. W. Harris, T. Michalowski, in *Asteroids III*, W. F. Bottke, A. Cellino, P. Paolicchi, R. Binzel, Eds. (Univ. of Arizona Press, Tucson, AZ, 2002), pp. 113–122.
8. W. F. Bottke, D. Vokrouhlický, D. P. Rubincam, M. Broz, in *Asteroids III*, W. F. Bottke, A. Cellino, P. Paolicchi, R. Binzel, Eds. (Univ. of Arizona Press, Tucson, AZ, 2002), pp. 395–408.
9. W. F. Bottke, D. Vokrouhlický, D. P. Rubincam, D. Nesvorný, *Annu. Rev. Earth Planet. Sci.* **34**, 157 (2006).
10. D. Vokrouhlický, D. Capek, M. Kaasalainen, S. J. Ostro, *Astron. Astrophys.* **414**, L21 (2004).
11. D. Capek, D. Vokrouhlický, *Icarus* **172**, 526 (2004).
12. P. A. Taylor *et al.*, *Science* **316**, 274 (2007); published online 8 March 2007 (10.1126/science.1139038).
13. See supporting material on *Science* Online.
14. R. C. Taylor, in *Asteroids*, T. Gehrels, Ed. (Univ. of Arizona Press, Tucson, AZ, 1979), pp. 480–493.
15. D. Vokrouhlický, D. Capek, *Icarus* **159**, 449 (2002).
16. R. J. Whiteley, C. W. Hergenrother, D. J. Tholen, *Proc. ACM* **2002**, 473 (2002).

17. We thank all the staff at the observatories involved in this study for their support. This work was based on observations at the following observatories: ESO, Chile (PIDs 271.C-5023 and 073.C-0137); Ondrejov Observatory, Czech Republic (grant A3003204); Centro Astronómico Hispano Alemán (Calar Alto, Spain); Liverpool Telescope, La Palma (Canary Islands, Spain); Isaac Newton Group, La Palma; and Faulkes Telescope North (Maui, Hawaii). We also thank the referees for their helpful reviews. Supported by the Leverhulme Trust (S.C.L.), the UK Particle Physics and Astronomy Research Council (A.F.), the Grant Agency of the Czech Republic (P.P. and D.V.), NASA grant NNG04GN31G (P.A.T. and J.-L.M.), and Slovak Grant Agency for Science VEGA grant 1/3074/06 (A.G.). This work made use of the NASA/JPL HORIZONS ephemeris-generating program.

Supporting Online Material

www.sciencemag.org/cgi/content/full/1139040/DC1
Materials and Methods
Fig. S1
Tables S1 and S2
References

19 December 2006; accepted 23 February 2007
Published online 8 March 2007;
10.1126/science.1139040
Include this information when citing this paper.

Spin Rate of Asteroid (54509) 2000 PH5 Increasing Due to the YORP Effect

Patrick A. Taylor,[1]* Jean-Luc Margot,[1]* David Vokrouhlický,[2] Daniel J. Scheeres,[3] Petr Pravec,[4] Stephen C. Lowry,[5] Alan Fitzsimmons,[5] Michael C. Nolan,[6] Steven J. Ostro,[7] Lance A. M. Benner,[7] Jon D. Giorgini,[7] Christopher Magri[8]

Radar and optical observations reveal that the continuous increase in the spin rate of near-Earth asteroid (54509) 2000 PH5 can be attributed to the Yarkovsky-O'Keefe-Radzievskii-Paddack (YORP) effect, a torque due to sunlight. The change in spin rate is in reasonable agreement with theoretical predictions for the YORP acceleration of a body with the radar-determined size, shape, and spin state of 2000 PH5. The detection of asteroid spin-up supports the YORP effect as an explanation for the anomalous distribution of spin rates for asteroids under 10 kilometers in diameter and as a binary formation mechanism.

Theory predicts an evolution of the spin state of a small solar system body as a result of the absorption and asymmetric re-emission of sunlight, the so-called YORP effect. The resultant radiation torques are thought to realign the spin vector while changing the spin rate of the object (*1*). Lowry *et al.* (*2*) report an increase in the spin rate of 2000 PH5. Here we present, with radar and optical observations and modeling of 2000 PH5, the best evidence to date that the YORP effect is responsible for changing the spin rate of an asteroid.

For objects with finite thermal conductivity, especially fast-rotating asteroids <1 km in diameter that lack regolith, YORP torques tend to force the spin vector to 0° or 180° obliquity (parallel or antiparallel to the orbit normal) and cause the spin rate to increase or decrease with equal probability (*3*) on time scales proportional to the square of the diameter D (*1*). Therefore, YORP may explain the observed excess of slow and rapid rotators among asteroids <10 km in diameter (*4*). Continuous spin-up by the YORP effect could result in a binary system from the shedding of mass as centrifugal forces overcome self-gravity and internal strength. Thus, along with spin-up from close planetary encounters (*5*–*8*) and subcatastrophic collisional fission (*9*), the YORP effect may be responsible for producing a fraction of the near-Earth asteroid binary systems (*10*).

Near-Earth asteroid (54509) 2000 PH5, hereafter referred to as PH5, was discovered by the Massachusetts Institute of Technology Lincoln Laboratory's near-Earth asteroid search program (LINEAR) (*11*) on 3 August 2000 at a geocentric distance of 0.04 astronomical units (AU). PH5 (semimajor axis a = 1.00 AU, eccentricity e = 0.23, inclination i = 1.8°) (fig. S1) is one of only a handful of objects known to be co-orbital companions of Earth (*12*–*14*). Annual close approaches from 2001 to 2005, as close as 5 lunar distances, were conducive to radar observations and allow us to present a spin-state description and detailed shape model (*15*) of PH5.

We conducted radar observations of PH5 (table S1) using the 70-m antenna and 450 kW, 3.5 cm wavelength transmitter at Goldstone on 27–28 July 2001 (*16*) and the 305-m antenna and 900 kW, 12.6 cm wavelength transmitter at Arecibo on 27–28 July 2004 and 24–26 July 2005. The radar echo is Doppler broadened by the rotation of the target (*17*), and the amount of broadening constrains the spin axis. Daily sums of Doppler-only spectra (fig. S2) determine the radar reflection properties of PH5 (table S2), which are similar to terrestrial planet surfaces (*18*).

Range-Doppler images (*19*) constrain the shape by resolving the radar echo in two orthogonal dimensions: distance from the observer and rotational Doppler shift. High-resolution images of PH5 from Arecibo (Fig. 1, first and fourth columns) with 7.5 m (0.05 μs) resolution reveal an echo 60 to 75 m deep, as well as an array of leading-edge features: convex, linear, and concave, as PH5 rotates. Visual inspection of the range-Doppler images suggests a rotation period of ~12 min, consistent with light-curve observations (*2*). The observing geometries during the 2001 and 2004 observations, which produced the most useful imagery, allow for ~75% surface coverage.

The limb-to-limb bandwidths of Doppler-only spectra (*20*) covering a full rotation of the target produce a bandwidth curve (fig. S3) whose amplitude variation is due to the changing breadth of the rotating nonspherical target on the sky. The mean bandwidth grows from 2001 to 2005, so the line of sight was moving away from the spin axis (*21*). Fits to individual Doppler-only spectra from 2001, 2004, and 2005 with simple ellipsoid and spherical harmonic shape models (*22*) constrain the spin vector to lie within 10° of (180°, –85°) in J2000 ecliptic coordinates at an

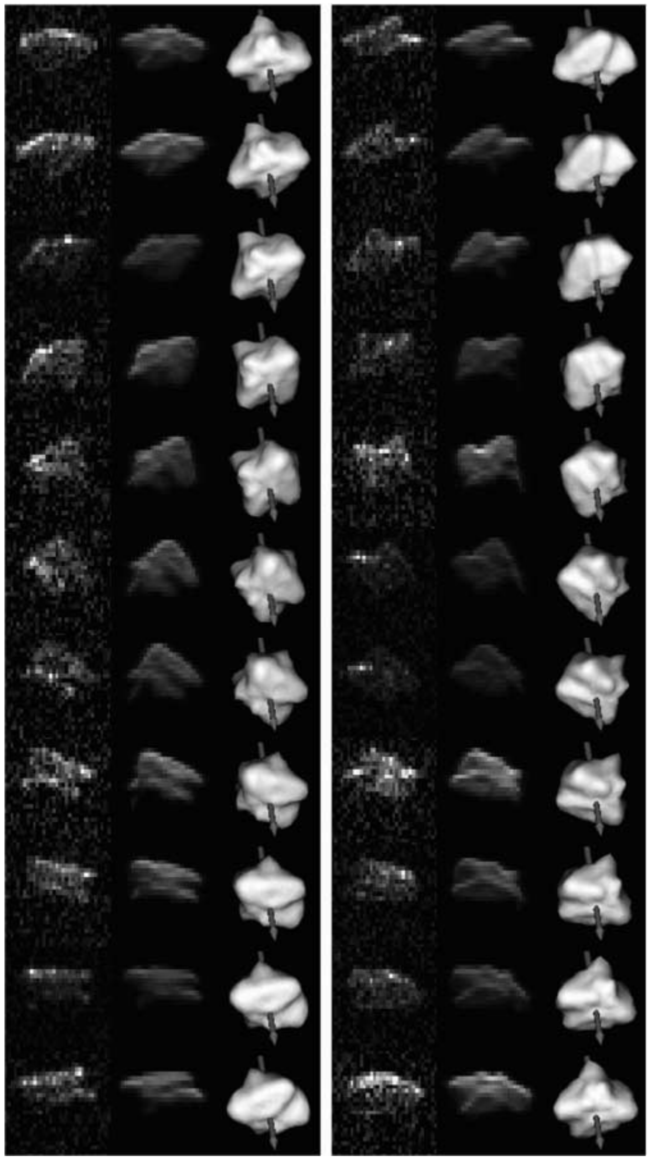

Fig. 1. Range-Doppler images (columns 1 and 4) obtained at Arecibo on 28 July 2004, covering one rotation of PH5, along with the corresponding shape model fits to the images (columns 2 and 5), and the plane-of-sky views (columns 3 and 6) of PH5 during the observations. Each 180-m by 180-m frame is separated by ~15° in rotation phase. Radar illumination is from the top of the frame. Range increases from top to bottom, and Doppler frequency increases from left to right; therefore, the rotation of the target appears counterclockwise. Time increases down the left side, then down the right side. The arrow through the plane-of-sky frames indicates the spin vector of PH5.

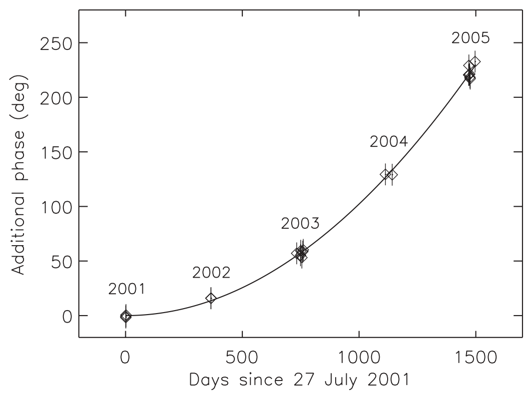

Fig. 2. Additional rotation phase required to link 20 optical light curves (*2*) from 2001 to 2005 using a shape model with pole (180°, –85°) fit to the 2001 light-curve data. The fitted curve is quadratic in time: $0.5\,\dot{\omega}t^2$, where $\dot{\omega}$ is the rate of change of the spin rate and t is time since the initial epoch of 0^h UT on 27 July 2001. Phases have conservative uncertainties of 10° because of their dependence on the exact shape and orientation of the asteroid.

[1]Department of Astronomy, Cornell University, Ithaca, NY 14853–6801, USA. [2]Institute of Astronomy, Charles University, V Holesovickách 2, 18000 Prague 8, Czech Republic. [3]Department of Aerospace Engineering, University of Michigan, 1320 Beal Avenue, Ann Arbor, MI 48109–2140, USA. [4]Astronomical Institute, Academy of Sciences of the Czech Republic, Fricova 1, CZ-25165 Ondrejov, Czech Republic. [5]School of Mathematics and Physics, Queen's University Belfast, Belfast BT7 1NN, UK. [6]Arecibo Observatory, HC3 Box 53995, Arecibo, PR 00612, USA. [7]Jet Propulsion Laboratory, California Institute of Technology, Pasadena, CA 91109–8099, USA. [8]University of Maine at Farmington, 173 High Street, Preble Hall, Farmington, ME 04938, USA.

*To whom correspondence should be addressed. E-mail: ptaylor@astro.cornell.edu (P.A.T.); jlm@astro.cornell.edu (J.L.M.)

obliquity of 173° from the orbit normal. This retrograde pole is adopted for shape modeling and translating between the observed light curve and intrinsic sidereal periods in the light-curve analysis (*2*). A prograde pole fits the observed bandwidths equally well but cannot fit bandwidth curves and light curves simultaneously.

A change in sidereal spin rate is necessary to fit the radar data over time. However, light-curve data alone provide a more accurate determination of the required change than does analysis of the range-Doppler imagery. To produce initial conditions for the spin state of our most detailed shape model, we fit synthetic light curves based on a simple spherical harmonic shape model to the 2001 light-curve data (*2*), which consist of three epochs over 24 hours, a time frame over which the change in spin rate is negligible. We then include the remaining light-curve data from 2002 to 2005 (*2*), allowing for an arbitrary phase shift for each light curve to match the phase of the shape model's synthetic light curves. The resulting phase shifts (Fig. 2) necessary to link the light curves are well fit by a quadratic function in time; in other words, the spin rate is increasing linearly with time. The use of a linear change in the spin rate rather than a constant spin rate yields improvement by a factor of ten in the reduced χ^2 value of a spherical harmonic fit to the entire collection of light-curve data.

For pole coordinates of (180°, –85°), the sidereal spin rate necessary to fit the light curve data are 42582.41 ± 0.02 deg/day (12.17-min period) at the initial epoch of 0^h UT on 27 July 2001, and the necessary change in spin rate is $(2.0 \pm 0.2) \times 10^{-4}$ deg/day^2. This determination of a continuous increase in spin rate precisely matches the discrete spin-period changes observed in (*2*). The fractional change in spin period is -1.72×10^{-6} (±10%) per year. Accelerations determined by this method for poles less than 10° from (180°, –85°) lie within 8% of the nominal acceleration, indicating relative insensitivity of the acceleration to precise pole location.

The shape models (*22*) of PH5 are 288-vertex polyhedra with 572 triangular facets giving the models 12° resolution in longitude, twice the amount PH5 rotated by during the exposure time for each range-Doppler image. We produced a family of models with a range of surface "roughness" based upon large-, medium-, and small- scale topography (*22*) to determine both the shapes that best fit the combined radar and light-curve data and how roughness affects the YORP acceleration calculations. All models produced have similar silhouettes, with much of the variation coming from the smoothness of the surface and the length of the shortest principal axis of inertia. The best PH5 shape model shows very good agreement with all range-Doppler images, reproducing the various convex, linear, and concave leading edges of the echoes (Fig. 1). The shape of PH5 (fig. S4) is distinguished by its flattened northern hemisphere with a linear edge and prominent concavity that are clearly visible in the radar images.

Table 1. Summary of shape models and predictions for the change in spin period due to the YORP effect. Shape A (rough) is the best-fit shape model depicted in Fig. 1, and the other shape models sample the 1-σ formal uncertainty region for the fit. "Smooth" and "rough" describe the amount of facet-scale topography the shape models allow. *a*, *b*, and *c* are the extents of the shape model along the principal axes of inertia. *D* is the diameter of a sphere with the same volume as the shape model. The YORP predictions are given by the factor by which they overestimate the observed change in spin period. Shape models with smoother surfaces result in predicted changes in spin period more consistent with observation than do rough surfaces, which provide better fits to the radar and light-curve data. Several factors could account for the discrepancy between observed and predicted values.

Shape	Type	*a*/*b*/*c* (m)	*D* (m)	$\Delta P/P_0$ per year factor	
				Model 1 (*3*)	Model 2 (*26*)
A	Smooth	150/128/93	114.2	2.86	3.72
	Rough	149/134/96	112.8	6.18	6.03
B	Smooth	149/130/91	113.2	2.95	3.36
	Rough	147/132/91	111.7	4.56	4.89
C	Smooth	149/129/97	115.1	2.63	3.24
	Rough	149/131/99	113.0	4.74	5.14
			Observed $\Delta P/P_0$ per year (2) = -1.72×10^{-6}		

The phase agreement between the rotating model and the entire set of range-Doppler images, as well as the ability to link the light curves from the 4-year optical photometry campaign (*2*), is due to the inclusion of a linear change in the intrinsic spin rate of PH5 (*23*). Harder to reproduce is the large amplitude of the PH5 light curves (fig. S5). The discrepancy may be due to unresolved topography, shadowing effects from concavities, albedo variations, or deficiencies in the photometric model used in the shape modeling software.

The rapid rotation of PH5, the increasing spin rate, and the near-180° obliquity are consistent with simulations of a body subjected to YORP torques (*3*). YORP torques can change the spin state of PH5 on less than million-year time scales (*2*), shorter than the dynamical (*2*, *24*) and collisional lifetimes (*25*) of about 10 million and 1 billion years, respectively, that would reorient the spin vector or disrupt the asteroid. Despite the repeated close encounters between PH5 and Earth, planetary tidal torques are not strong enough (*2*) to cause the observed change in spin rate. Without other plausible causes, the YORP effect is the most viable mechanism for explaining the observations.

Using the PH5 spin state and shape models, two independent YORP acceleration models (*3*, *26*) predict changes in spin rate, in terms of the fractional change in spin period ($\Delta P/P_0$) per year, 2 to 7 times as large as those observed (Table 1). Smooth models, those with less facet-scale topography, produce changes in spin rate closer by a factor of 2 to the observed value as models with rougher surfaces. Several factors may account for the discrepancy between observed and theoretical values. The incomplete surface coverage by radar of PH5's irregular shape undoubtedly affects the accuracy of the shape model. Mismodeled morphology results in erroneous YORP torque values and accelerations that could cause errors even greater than the factor of 2 seen between smooth and rough models. Unresolved surface characteristics much finer than the radar resolution may also be very important for accurate torque calculations. Furthermore, we assume a bulk density ρ of 2.5 g/cm^3. Because $\Delta P/P_0$ per year scales as $(\rho D^2)^{-1}$, a combination of higher density and larger size could reduce the discrepancy. Deficiencies in the YORP simulations, including the thermal model formulation and uncertainties in key thermal parameters and surface-scattering properties, may also play a role. Simulations assume an ideal Lambertian scattering surface; in general, a non-ideal surface would produce a result more consistent with observation. Although PH5 has significantly nonzero thermal inertia (*27*), trials of surface thermal conductivities between 0.005 and 0.05 W/m/K show no appreciable change in results, as expected (*3*, *26*). Altogether, a combination of incomplete surface coverage and assumptions about density, thermal parameters, and scattering properties are likely responsible for the discrepancy we find. The order-of-magnitude agreement between observation and theory provides the best evidence to date that the YORP effect acts upon small solar-system bodies.

The observation of a continuously increasing asteroid spin rate and the reasonable agreement with theoretical models support the YORP effect as an important process for altering the spin state of small solar system bodies. YORP may therefore explain several puzzling issues in asteroid dynamics, including the observed spin-rate distribution of asteroids <10 km in diameter and the production of binary systems.

References and Notes

1. D. P. Rubincam, *Icarus* **148**, 2 (2000).
2. S. C. Lowry *et al.*, *Science* **316**, 272 (2007); published online 8 March 2007; 10.1126/science.1139040.
3. D. Capek, D. Vokrouhlický, *Icarus* **172**, 526 (2004).
4. P. Pravec, A. W. Harris, *Icarus* **148**, 12 (2000).
5. W. F. Bottke, H. J. Melosh, *Nature* **381**, 51 (1996).

6. E. Asphaug, W. Benz, *Icarus* **121**, 225 (1996).
7. D. C. Richardson, W. F. Bottke, S. G. Love, *Icarus* **134**, 47 (1998).
8. J. L. Margot *et al.*, *Science* **296**, 1445 (2002).
9. S. J. Weidenschilling, P. Paolicchi, V. Zappalà, in *Asteroids II*, R. P. Binzel, T. Gehrels, M. S. Matthews, Eds. (Univ. of Arizona Press, Tucson, AZ, 1989), pp. 643–658.
10. W. F. Bottke, D. Vokrouhlický, D. P. Rubincam, M. Broz, in *Asteroids III*, W. F. Bottke, P. Paolicchi, R. P. Binzel, A. Cellino, Eds. (Univ. of Arizona Press, Tucson, AZ, 2002), pp. 395–408.
11. G. H. Stokes, J. B. Evans, H. E. M. Viggh, F. C. Shelly, E. C. Pearce, *Icarus* **148**, 21 (2000).
12. P. Wiegert *et al.*, American Geophysical Union, Fall Meeting 2002, abstr. #P11A-0352 (2002).
13. J. L. Margot, P. D. Nicholson, *AAS/Division of Dynamical Astronomy Meeting* **34** (2003).
14. R. Brasser *et al.*, *Icarus* **171**, 102 (2004).
15. S. Hudson, *Remote Sensing Rev.* **8**, 195 (1993).
16. J. L. Margot *et al.*, *Bull. Am. Astron. Soc.* **35**, 960 (2003).
17. The Doppler broadening of the radar echo due to rotation of the target is $B = (4\pi D/\lambda P)\sin\alpha$, where B is the limb-to-limb bandwidth of the echo, D is the target diameter producing the Doppler shift at the current viewing geometry and rotation phase, λ is the radar wavelength, P is the spin period of the target, and α is the inclination of the spin axis to the line of sight.
18. S. J. Ostro, *Rev. Mod. Phys.* **65**, 1235 (1993).
19. Resolution in time delay, and equivalently range, is achieved by transmitting a time-dependent signal and analyzing the received signal according to arrival time. The time increment τ used in the transmitted signal yields a range resolution $c\tau/2$, where c is the speed of light.
20. We typically define the limb-to-limb bandwidth as the full width of the radar echo at the level of twice the root mean square (RMS) of the off-DC, off-target noise. The exception is the strong 2004 Arecibo data, for which we use 10 times the RMS as the threshold to avoid contributions from frequency sidelobes.
21. This assumes PH5 is a principal axis (PA) rotator where the spin axis remains fixed in inertial space and aligned with the axis of maximum moment of inertia. The spin axis of PH5 must then be oriented such that the angles it makes with the lines of sight satisfy the observed bandwidths (*17*). The damping time scale (*28*) to PA rotation for PH5 is of order 0.1 million years.
22. Materials and methods are available as supporting material on *Science* Online.
23. The spin state solution is also validated by the phase agreement of infrared lightcurves from the Spitzer Space Telescope with synthetic lightcurves produced with our shape (*27*).
24. B. Gladman *et al.*, *Science* **277**, 197 (1997).
25. W. F. Bottke Jr., M. C. Nolan, R. Greenberg, R. A. Kolvoord, in *Hazards Due to Comets and Asteroids*, T. Gehrels, M. S. Matthews, A. M. Schumann, Eds. (Univ. of Arizona Press, Tucson, AZ, 1994), pp. 337–357.
26. D. J. Scheeres, *Icarus* 10.1016/j.icarus.2006.12.015 (2007).
27. M. Mueller, A. W. Harris, *IAU General Assembly Abstracts* (2006), p. 95.
28. I. Sharma, J. A. Burns, C.-Y. Hui, *Mon. Not. R. Astron. Soc.* **359**, 79 (2005).

29. We thank the staffs of the Arecibo Observatory and the Goldstone Solar System Radar for their support in performing this research. The Arecibo Observatory is part of the National Astronomy and Ionosphere Center, which is operated by Cornell University under a cooperative agreement with NSF. Some of this work was performed at the Jet Propulsion Laboratory, California Institute of Technology, under contract with NASA. This material is based in part on work supported by NASA under the Science Mission Directorate Research and Analysis Programs. P.A.T. and J.L.M. were partially supported by NASA grant NNG04GN31G. The work of P.P. and D.V. was supported by the Grant Agency of the Czech Republic. D.J.S. acknowledges support from the NASA Planetary Geology and Geophysics Program. S.C.L. and A.F. acknowledge support from the Leverhulme Trust and PPARC, respectively. C.M. was partially supported by NSF grant AST-0205975. The International Astronomical Union has approved the name YORP for asteroid (54509) 2000 PH5.

Supporting Online Material
www.sciencemag.org/cgi/content/full/1139038/DC1
Methods
Figs. S1 to S5
Tables S1 and S2
References

19 December 2006; accepted 21 February 2007
Published online 8 March 2007;
10.1126/science.1139038
Include this information when citing this paper.

Analyses of Soft Tissue from *Tyrannosaurus rex* Suggest the Presence of Protein

Mary Higby Schweitzer,[1,2,3]* Zhiyong Suo,[4] Recep Avci,[4] John M. Asara,[5,6] Mark A. Allen,[7] Fernando Teran Arce,[4,8] John R. Horner[3]

We performed multiple analyses of *Tyrannosaurus rex* (specimen MOR 1125) fibrous cortical and medullary tissues remaining after demineralization. The results indicate that collagen I, the main organic component of bone, has been preserved in low concentrations in these tissues. The findings were independently confirmed by mass spectrometry. We propose a possible chemical pathway that may contribute to this preservation. The presence of endogenous protein in dinosaur bone may validate hypotheses about evolutionary relationships, rates, and patterns of molecular change and degradation, as well as the chemical stability of molecules over time.

It has long been assumed that the process of fossilization results in the destruction of virtually all original organic components of an organism, and it has been hypothesized that original molecules will be either lost or altered to the point of nonrecognition over relatively short time spans (well under a million years) (*1*–*7*). However, the discovery of intact structures retaining original transparency, flexibility, and other characteristics in specimens dating at least to the Cretaceous (*8*, *9*) suggested that, under certain conditions, remnant organic constituents may persist across geological time.

The skull, vertebrae, both femora and tibiae, and other elements of an exceptionally well-preserved *Tyrannosaurus rex* [MOR 1125 (*8*)] were recovered from the base of the Hell Creek Formation in eastern Montana (USA), buried within at least 1000 m^3 of medium-grained, loosely consolidated sandstone interfingered with fine-grained muds, interpreted as stream channel sediments. Demineralization of femur and tibia fragments revealed the preservation of fibrous, flexible, and apparently original tissues, as well as apparent cells and blood vessels (*8*), but the endogeneity and composition of these structures could not be ascertained without further analyses.

We present molecular and chemical (*10*) analyses of tissues remaining after partial demineralization (*11*) of the left and right femora and associated medullary bone (*12*) that would, in extant bone, represent the extracellular matrix (osteoid) dominated by collagen I (*13*). Because of its ordered structure as a triple helix (*14*, *15*), collagen I has unique characteristics that are highly conserved across taxa, making validation of its presence relatively straightforward. The molecular composition of collagen incorporates glycine, the smallest amino acid, at every helical turn. Therefore, an amino acid profile of collagen results in ~33% glycine content (*14*). This molecular structure also results in packing of microfibrils with a banded repeat of ~70 nm (*15*, *16*). Collagen also shows posttranslational hydroxylation of about half of all proline and some lysine residues; thus, the detection of hydroxyproline and hydroxylysine in extracts of organic material is viewed as strong evidence for the presence of collagen (*17*, *18*). Finally, collagen is identified by polyclonal or monoclonal antibody reactivity that can distinguish between collagen types (*19*). We focused on identifying collagen-like compounds because in addition to being abundant and easily identified by multiple

[1]Department of Marine, Earth and Atmospheric Sciences, North Carolina State University, Raleigh, NC 27695, USA. [2]North Carolina Museum of Natural Sciences, Raleigh, NC 27601, USA. [3]Museum of the Rockies, Montana State University, Bozeman, MT 59717, USA. [4]Image and Chemical Analysis Laboratory Facility, Department of Physics, Montana State University, Bozeman, MT 59717, USA. [5]Division of Signal Transduction, Beth Israel Deaconess Medical Center, Boston, MA 02115, USA. [6]Department of Pathology, Harvard Medical School, Boston, MA 02115, USA. [7]Department of Chemistry and Biochemistry, Montana State University, Bozeman, MT 59717, USA. [8]Center for Nanomedicine, Pulmonary and Critical Care Medicine, Department of Medicine, University of Chicago, Chicago, IL 60637, USA.

*To whom correspondence should be addressed. E-mail: schweitzer@ncsu.edu